First Observation of the $E2$ Nuclear-Resonance Effect in Antiprotonic Atoms

W. Kanert, F. J. Hartmann, H. Daniel, E. Moser, G. Schmidt, and T. von Egidy
Physik-Department, Technische Universität München, D-8046 Garching, Federal Republic of Germany

J. J. Reidy and M. Nicholas
University of Mississippi, University, Mississippi 38677

M. Leon
Los Alamos National Laboratory, Los Alamos, New Mexico 87545

H. Poth, G. Büche, A. D. Hancock, H. Koch, Th. Köhler, A. Kreissl, U. Raich, and D. Rohmann
Kernforschungszentrum Karlsruhe, Institut für Kernphysik, and Institut für experimentelle Kernphysik, Universität Karlsruhe, D-7500 Karlsruhe, Federal Republic of Germany

M. Chardalas and S. Dedoussis
Department of Nuclear Physics, University of Thessaloniki, Thessaloniki, Greece

M. Suffert
Centre de Recherches Nucléaires and Université Louis Pasteur, F-67037 Strasbourg, France

A. Nilsson
Research Institute for Physics, S-10450 Stockholm, Sweden
(Received 23 December 1985)

Antiprotonic x-ray spectra of ^{92}Mo, ^{94}Mo, ^{95}Mo, ^{98}Mo, and ^{100}Mo have been measured with Ge detectors. The $E2$ nuclear-resonance effect was observed for the first time in $\bar{p}$ atoms, yielding information on the "hidden" $n=5$, $l=4$ level of the $\bar{p}$-molybdenum atom. Strong interaction widths and shifts affecting the $7\rightarrow 6$ transition were determined and the effective $\bar{p}$-nucleon scattering length was deduced. A unique strong-coupling effect was established in $\bar{p}$-^{100}Mo.

PACS numbers: 36.10.−k, 13.75.Cs, 23.20.Qz

Antiprotonic atoms are successfully used to obtain information on the strong interaction between matter and antimatter at low energies. The strong interaction leads to a shift and to a broadening of the $\bar{p}$-atomic levels compared with the values calculated without strong interaction. These effects are best observed in the last antiprotonic transition which can be seen. The data are usually interpreted in terms of phenomenological $\bar{p}$-nucleus or $\bar{p}$-nucleon optical potentials and scattering lengths[1]; however, microscopic models[2] have been recently constructed.

An additional source of information on the antiproton-nucleus interaction is provided by the hadronic $E2$ nuclear-resonance effect,[3] which has previously been observed in pionic[4] and kaonic[5] atoms. This effect occurs when an atomic deexcitation energy matches a nuclear excitation energy and the electric quadrupole coupling induces configuration mixing. For $\bar{p}$-^{94}Mo and $\bar{p}$-^{100}Mo this effect was predicted some years ago.[3] The relevant levels for both isotopes are shown in Fig. 1.

In the case of ^{94}Mo the spacing between the antiprotonic $(n,l)=(7,6)$ and (5,4) levels (844.8 keV) is sufficiently close to the first $I^{\pi}=2^{+}$ nuclear excitation energy (871.1 keV) to allow configuration mixing of the $(7,6;I^{\pi}=0^{+})$ and $(5,4;I^{\pi}=2^{+})$ states. The ad-

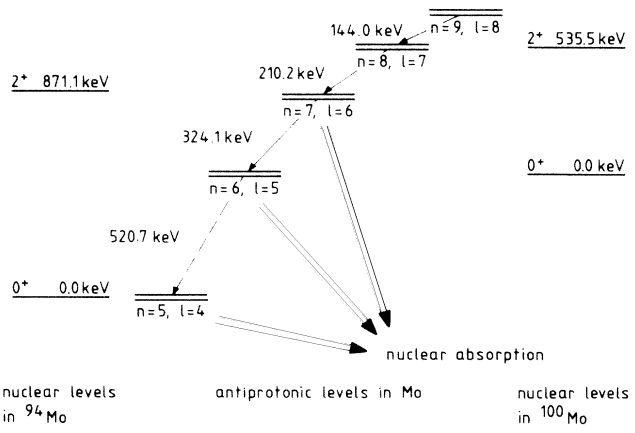

FIG. 1. Nuclear and $\bar{p}$-atomic levels in ^{94}Mo and ^{100}Mo relevant to the $E2$ resonance effect.

TABLE I. Relative intensities of relevant antiprotonic x-ray lines[a]; for normalization the intensity of the $11 \rightarrow 10$ was set to 100.

Transition	E (keV)	Target / Isotopic purity ^{92}Mo 98.3%	^{94}Mo 93.9%	^{95}Mo 95.4%	^{98}Mo 97.2%	^{100}Mo 96.0%
$11 \rightarrow 10$	76.0	100.0 ± 1.8	100.0 ± 1.7	100.0 ± 1.7	100.0 ± 1.6	100.0 ± 2.1
$(10 \rightarrow 9) + (13 \rightarrow 11)$	102.8	134.6 ± 2.1	136.0 ± 1.9	135.5 ± 1.9	132.8 ± 1.8	137.0 ± 2.5
$9 \rightarrow 8$	143.8	128.1 ± 2.4	127.4 ± 2.4	128.5 ± 2.5	128.6 ± 2.5	128.7 ± 3.2
$8 \rightarrow 7$	210.0	132.0 ± 2.5	124.7 ± 2.3	120.2 ± 2.3	121.8 ± 2.2	5.4 ± 0.7
$7 \rightarrow 6$	324.1	33.9 ± 1.3	11.4 ± 1.5	22.9 ± 1.6	14.7 ± 1.4	11.1 ± 1.5

[a]Not corrected for isotopic composition.

mixture of the lower antiprotonic level causes an increase of the strong absorption width for the upper level which reduces the $(n=7) \rightarrow (n=6)$ x-ray intensity compared with that in ^{92}Mo; in the latter this is ruled out because the excitation energy of the first nuclear 2^+ state is 1.51 MeV. From the reduction one can deduce the width of the "hidden" (5,4) level. This level is not reached directly in the antiprotonic x-ray cascade as a result of the strong $\bar{p}$ absorption in the $n=6$ state.

In ^{100}Mo the spacing between the (8,7) and (6,5) levels (534.3 keV) is very close to the first $I^{\pi}=2^+$ nuclear excitation energy (535.5 keV), which leads to a unique strong coupling[3] between the $(8,7;0^+)$ and the $(6,5;2^+)$ levels. As a result, the $8 \rightarrow 7$ line is predicted to be very strongly attenuated. Furthermore, the usual fine-structure doublet of the $9 \rightarrow 8$ line is converted into a quartet (if we neglect weak spin-flip components). The various components are not resolved, but the $9 \rightarrow 8$ line is broadened.

The experiment was performed by use of the slow antiproton beam of the Low-Energy Antiproton Ring at CERN. The incoming antiprotons (momentum 300 and 200 MeV/c for various runs), identified by a scintillation-counter telescope, were focused on the target and stopped therein, after having been slowed down in a moderator. As a result of the high quality of the beam, the focal-area diameter (FWHM) was only about 12 mm and the width of the range curve less than 100 mg/cm^2 polyethylene. The $\bar{p}$ flux was mostly between 10^4 and 10^5 $\bar{p}$ s^{-1}. Five targets were measured: ^{92}Mo, ^{94}Mo, ^{95}Mo, ^{98}Mo, and ^{100}Mo. The targets consisted of highly enriched metal foils with areas of approximately 7.5 cm^2 and areal densities of 100 mg/cm^2 (Table I). The x- and γ-ray spectra were measured with several Si(Li) and Ge detectors. The spectra relevant for this work were obtained with two high-purity Ge detectors of dimensions 2 cm^2 × 0.7 cm (a) and 5 cm^2 × 1.3 cm (b), in-beam resolution 0.57 keV and 0.80 keV, respectively, at 75 keV. The angle between detector axis and target normal was 40°. Parts of the spectra as recorded by Ge detector (b) are displayed in Fig. 2. The directly observed intensities were corrected for detector efficiency and target self-absorption. Table I provides relative intensities of relevant transitions; the errors include the errors of the corrections. Transitions not influenced by the resonance effect have similar intensities in all isotopes.

Considerable strong-interaction absorption from the (7,6) level takes place even without the resonance effect, leading to a reduced intensity of the $7 \rightarrow 6$ transition. The strong-interaction width $\Gamma_{SI}(7,6)$ was derived from the experimental intensities of the transitions populating (I_{pop}) and depopulating (I_{dep}) the

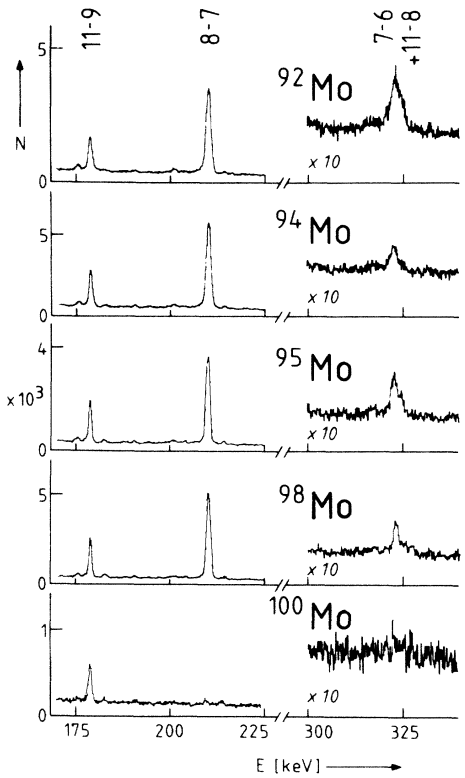

FIG. 2. Parts of the antiprotonic x-ray spectra of ^{92}Mo, ^{94}Mo, ^{95}Mo, ^{98}Mo, and ^{100}Mo; counts per channel vs energy E, one channel corresponding to 0.13 keV for ^{92}Mo and ^{94}Mo, and to 0.16 keV for ^{95}Mo, ^{98}Mo, and ^{100}Mo.

TABLE II. Summary of experimental and calculated results for levels of interest in some Mo isotopes.

$E_{\text{nuclear}}(I^{\pi})$ (MeV)	^{92}Mo 1.51(2$^+$)	^{94}Mo 0.871(2$^+$)	^{95}Mo 0.948($\frac{9}{2}^+$)	^{98}Mo 0.787(2$^+$)
$\Gamma_{SI}(7,6)$, expt (eV)	19.5 ± 1.2	68.9 ± 10.3	28.5 ± 2.6	47.9 ± 5.3
$\Gamma^0_{SI}(7,6)$, calc[a] (eV)	19.5(21.2)	20.9(22.7)	21.3(23.2)	23.4(25.4)
$\Gamma_{ind}(7,6)$, expt (eV)		48.0 ± 10.4	7.2 ± 2.9	24.5 ± 5.4
$\Gamma_{ind}(7,6)$, calc[a] (eV)		37.4(46.0)	4.6(5.9)	20.5(23.0)
$\Gamma^0_{SI}(5,4)$, expt (keV)		42.5 ± 9.2	49.9 ± 19.8	45.1 ± 10.0
$\Gamma^0_{SI}(5,4)$, calc[a] (keV)		32.2(40.8)	32.4(41.2)	33.3(42.4)
$\Gamma_{SI}(6,5)$, expt (keV)	1.4 ± 0.3	2.3 ± 0.9	1.9 ± 0.4	2.3 ± 0.7
$\Gamma_{SI}(6,5)$, calc[a] (keV)	1.4(1.6)	1.4(1.7)	1.5(1.7)	1.6(1.9)
$-\epsilon_{SI}(6,5)$, expt (keV)	0.46 ± 0.08	0.64 ± 0.22	0.74 ± 0.12	0.55 ± 0.16
$-\epsilon_{SI}(6,5)$, calc[a] (keV)	0.46(0.27)	0.49(0.30)	0.51(0.31)	0.55(0.34)

[a]Calculated with phenomenological optical potential (Ref. 10) using $\bar{a} = (0.25 + 3.05i)$ fm and, in parentheses, with $\bar{a} = (1.53 + 2.50i)$ fm.

(7,6) level, and from the radiative width $\Gamma_{rad}(7,6)$ ($= 5.78$ eV for ^{92}Mo) calculated with a cascade code[6] (including the Fried-Martin factor[7]), according to the relation[8]

$$\Gamma_{SI}(7,6) = \Gamma_{rad}(7,6)(I_{pop}/I_{dep} - 1).$$

The resulting strong-interaction width for ^{92}Mo is $^{92}\Gamma_{SI}(7,6) = 19.5 \pm 1.2$ eV.

In the same way $\Gamma_{SI}(7,6)$ can be found for the resonant isotopes ^{94}Mo, ^{95}Mo, and ^{98}Mo. The results, corrected for the isotopic composition of the targets, are summarized in Table II. These widths can be written as the sum of an intrinsic part and an induced part which comes from the mixing with the (5,4) level,[9]

$$^{A}\Gamma_{SI}(7,6) = {}^{A}\Gamma^0_{SI}(7,6) + {}^{A}\Gamma_{ind}(7,6).$$

$^{A}\Gamma^0_{SI}(7,6)$ was calculated with neglect of spin effects by integration of the Schrödinger equation with a fitted optical potential.[10] For the calculation we used a fit value for the effective $\bar{p}$-nucleon scattering length which reproduces the measured strong-interaction effects in ^{92}Mo: $\bar{a} = (0.25 \pm 3.05i)$ fm. Calculations were also made with $\bar{a} = (1.53 \pm 2.50i)$ fm, a value given by Batty.[11]

The induced width $\Gamma_{ind}(7,6)$ is related[3] to the strong-interaction width $\Gamma^0_{SI}(5,4)$ by

$$\Gamma_{ind}(7,6) = |a|^2 \Gamma^0_{SI}(5,4),$$

where a is the admixture coefficient, defined in Ref. 3. However, from the experiment one cannot determine the real part of the energy difference between the mixed levels and the imaginary part $\Gamma^0_{SI}(5,4)$ separately. By use of an admixture coefficient derived from optical-potential calculations, values were deduced for $\Gamma^0_{SI}(5,4)_{expt}$. They are summarized in Table II, together with theoretical values. The agreement is reasonable. The strong-interaction widths $^{A}\Gamma_{SI}(6,5)$ and the shifts $^{A}\epsilon_{SI}(6,5)$ of the level (6,5) are also given. The shift ϵ_{SI} is defined by $\epsilon_{SI} = E_{expt} - E_{em}$, where E_{expt} is the experimental value for the transition energy and E_{em} is the energy calculated without strong interaction.[12] As the shift of the upper level is negligible, ϵ_{SI} can be ascribed to the lower level. The experimental values agree with optical-potential calculations. No isotope effect can be seen within the experimental errors. The value[11] $\bar{a} = (1.53 + 2.50i)$ fm is in agreement with the measured widths Γ_{SI}, but not with the measured shifts ϵ_{SI}.

In the case of ^{100}Mo the observed attenuation of the $8 \rightarrow 7$ line, 0.998 ± 0.006, may be compared with the predicted value[3] of 0.98. The predicted strong coupling is further corroborated by the evident broadening of the $9 \rightarrow 8$ line and the wings on both sides. With use of the double-pole formula of Ref. 3 [Eq. (12)] a

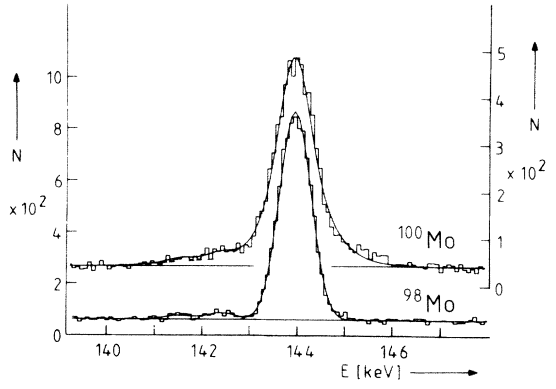

FIG. 3. The antiprotonic $9 \rightarrow 8$ x-ray line in ^{100}Mo and ^{98}Mo. The fitted curves are obtained by folding the experimental Gaussian line shape with the special structure given in Ref. 3 for ^{100}Mo and with the fine-structure splitting for ^{98}Mo. Two additional γ lines at 141.6 and 142.4 keV are included in the fit in both cases. The upper curve gives the total fit. The contribution of the antiprotonic line under the γ lines is indicated.

good fit (reduced χ^2 value of 1.2) was obtained. Figure 3 shows the $9 \rightarrow 8$ line together with the fit and, for comparison, the corresponding line in ^{98}Mo; both were measured with Ge detector (a).

In summary, the $E2$ resonance effect in antiprotonic atoms which is due to the coupling between atomic and nuclear states has been observed for the first time. The present data provide inforation on the "hidden" ($n=5, l=4$) level of $\bar{p}$-Mo. A unique strong coupling in $\bar{p}$-^{100}Mo has been established. In view of our results we conclude that the $E2$ nuclear-resonance effect is probably a frequent phenomenon and has to be considered whenever strong-interaction information is extracted from antiprotonic atoms.

We wish to thank G. Fricke and L. Schellenberg for providing the even-A Mo targets and H. Angerer, H. Hagn, P. Stoeckel, and J. Hauth for technical assistance. We appreciate the hospitality of CERN and the cooperation of the Low-Energy Antiproton Ring staff providing the high-quality $\bar{p}$ beam. Financial support from the German Federal Ministry of Research and Technology and the U. S. National Science Foundation is gratefully acknowledged.

[1]H. Poth *et al.*, Nucl. Phys. **A294**, 435 (1978); C. J. Batty, Sov. J. Part. Nucl. **13**, 71 (1982) [Fiz. Elem. Chastits At. Yadra **13**, 164 (1982)], and references cited therein.

[2]A. M. Green, W. Stepien-Rudzka, and S. Wycech, Nucl. Phys. **A399**, 307 (1983); T. Suzuki and H. Narumi. Nucl. Phys. **A426**, 413 (1984).

[3]M. Leon, Nucl. Phys. **A260**, 461 (1976).

[4]J. N. Bradbury *et al.*, Phys. Rev. Lett. **34**, 303 (1975); J. J. Reidy *et al.*, Phys. Rev. **C32**, 1646 (1985).

[5]G. L. Godfrey, G. K. Lum, and C. E. Wiegand, Phys. Lett. **61B**, 45 (1976); C. J. Batty *et al.*, Nucl. Phys. **A296**, 361 (1978).

[6]F. J. Hartmann, computer program CASH (unpublished).

[7]Z. Fried and A. D. Martin, Nuovo Cimento **29**, 574 (1963).

[8]H. Koch *et al.*, Phys. Lett. **29B**, 140 (1969).

[9]M. Leon, Phys. Lett. **50B**, 425 (1974).

[10]Computer program PIKACAS (unpublished).

[11]C. J. Batty, Nucl. Phys. **A372**, 433 (1981).

[12]E. Borie and G. A. Rinker, Rev. Mod. Phys. **54**, 67 (1982).